

## Quantitative Footprinting Analysis Using a DNA-Cleaving Metalloporphyrin Complex<sup>†</sup>

James C. Dabrowiak,\* Brian Ward, and Jerry Goodisman

Department of Chemistry, Syracuse University, Syracuse, New York 13244-1200

Received October 13, 1988; Revised Manuscript Received December 9, 1988

**ABSTRACT:** The results of quantitative footprinting studies involving the antiviral agent netropsin and a DNA-cleaving cationic metalloporphyrin complex are presented. An analysis of the footprinting autoradiographic spot intensities using a model previously applied to footprinting studies involving the enzyme DNase I [Ward, B., Rehfuess, R., Goodisman, J., & Dabrowiak, J. C. (1988) *Biochemistry* 27, 1198-1205] led to very low values for netropsin binding constants on a restriction fragment from pBR-322 DNA. In this work, we show that, because the porphyrin binds with high specificity to DNA, it does not report site loading information in the same manner as does DNase I. We elucidate a model involving binding equilibria for individual sites and include competitive binding of drug and porphyrin for the same site. The free porphyrin and free drug concentrations are determined by binding equilibria with the carrier (calf thymus DNA) which is present in excess and acts as a buffer for both. Given free porphyrin and free netropsin concentrations for each total drug concentration in a series of footprinting experiments, one can calculate autoradiographic spot intensities in terms of the binding constants of netropsin to the various sites on the 139 base pair restriction fragment. The best values of these binding constants are determined by minimizing the sum of the squared differences between calculated and experimental footprinting autoradiographic spot intensities. Although the determined netropsin binding constants are insensitive to the value assumed for the porphyrin binding constant toward its highest affinity sites, the best mean-square deviation between observed and calculated values,  $D$ , depends on the choice of (average) drug binding constant to carrier DNA,  $K_d$ . Since  $D$  as a function of  $K_d$  passes through a clear minimum, we were able to determine this parameter as well. The study demonstrates that the specificity of probe binding to DNA is an important factor influencing the reporting of site occupancy by drug in the quantitative footprinting experiment.

In the footprinting experiment, a ligand is allowed to bind to a DNA molecule before exposure of the ligand-DNA complex to a cleavage agent. From the way in which the amount of a particular DNA oligomer produced in the digest changes with the amount of ligand added, one can determine whether ligand binds at a specific site on the DNA lattice. In a quantitative footprinting experiment, one attempts to extract values for the equilibrium binding constants of the ligand by analyzing the concentrations of DNA oligomers as a function of ligand concentration and sequence.

The most commonly used footprinting agent or probe is the DNA hydrolytic enzyme DNase I. Ackers and co-workers (Brenowitz et al., 1986a,b; Senear et al., 1986; Carey, 1988) have recently reported that this enzyme yields valid individual-site isotherms for protein-DNA interactions. While the extension of quantitative footprinting techniques to drugs and other small ligands appears straightforward, the low binding specificities and reduced affinities of these agents complicate the extraction of binding constants from footprinting data.

In recent quantitative studies involving the antiviral agent netropsin, a 139 base pair restriction fragment of pBR-322 DNA, and DNase I, we demonstrated that it is possible to obtain drug binding constants as a function of sequence from footprinting data (Ward et al., 1988a). After addressing DNase I redistribution effects due to drug binding (Ward et al., 1988b) and site exclusions due to overlapping binding sites on DNA, we analyzed the autoradiographic data associated with binding events as well as enhancements, obtaining values

for a number of affinity constants for netropsin. The results indicated that, although the high-affinity drug sites are all of type (A·T)<sub>4</sub>, the presence of the sequence 5'-TA-3', which produces a distortion within the site, (Chuprina, 1987) discourages netropsin binding to DNA.

Since quantitative footprinting analysis is certain to have a major role in the design and synthesis of new generations of sequence-specific drugs (Hurley & Boyd, 1987), it is important to more clearly define the scope and limitations of the new method. In this work, we examine how the cleavage characteristics of the probe affect reporting of valid binding information in the footprinting experiment. We carried out quantitative footprinting studies of netropsin bound to a 139 base pair restriction fragment, using, instead of DNase I as a cleaving agent, the DNA-cleaving cationic manganese-porphyrin complex MnT4MPyP. The different cleavage properties associated with the porphyrin lead to substantial differences from the previous work. Unlike DNase I, which cleaves at many sites on DNA, MnT4MPyP prefers to cleave at trinucleotide sequences containing only the bases adenine and thymine, i.e., (A·T)<sub>3</sub> (Ward et al., 1986, 1987). In addition to altered specificity, DNase I and MnT4MPyP exhibit different binding and cleavage mechanisms. While the enzyme binds to a well-formed minor groove (Suck et al., 1988), the metal complex interacts in what appears to be a melted or partially melted region of DNA (Raner et al., 1988, 1989; Geacintov et al., 1987). Activation of the porphyrin is believed to proceed through a high-valent oxo intermediate which attacks the deoxyribose group, ultimately producing a strand break in the polymer (Ward et al., 1986; Bortolini et al., 1986; Groves & Nemo, 1983a,b). This behavior contrasts with that

<sup>†</sup> This work was supported by a grant from the American Cancer Society, NP-681.

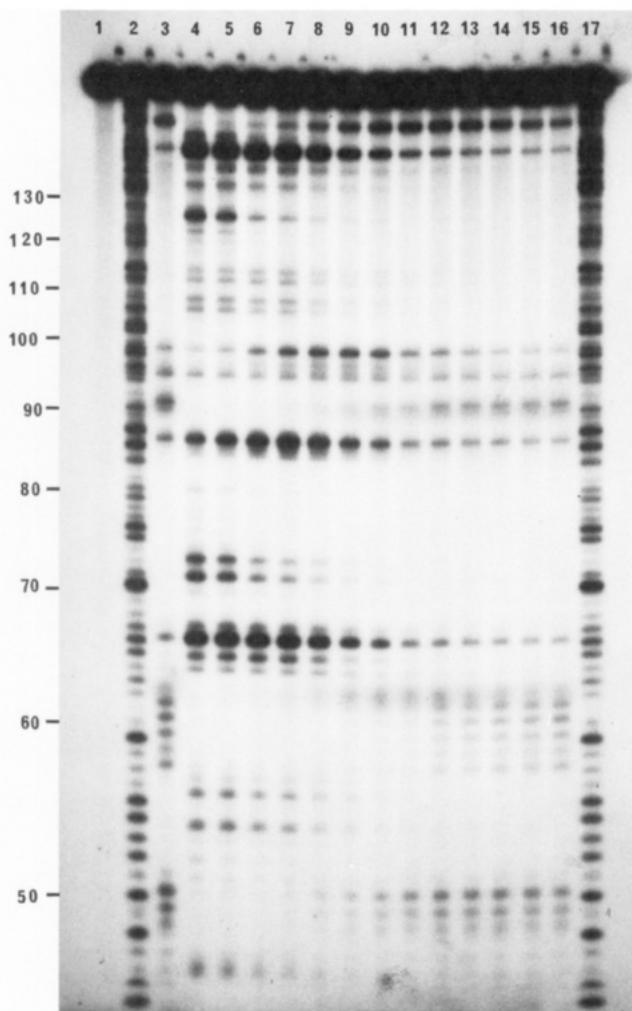


FIGURE 1: Photograph of autoradiographic data of the netropsin-139-mer interaction as probed with MnT4MPyP/oxone. Lane 1, no porphyrin control; lanes 2 and 17, DNase I cleavage of the 139-mer in the absence of netropsin; lanes 4-15, cleavage by MnT4MPyP/oxone in the presence of various concentrations of netropsin. The drug concentrations used (lane 4 highest, lane 15 lowest) can be found under Materials and Methods.

of DNase I, which, through a calcium-dependent reaction, catalyzes the hydrolysis of the phosphodiester backbone of DNA (Suck et al., 1988).

#### MATERIALS AND METHODS

The 139 base pair *HindIII*/*NciI* restriction fragment obtained from pBR-322 DNA was 3' end labeled at position 33 with [ $\alpha$ - $^{32}$ P]ATP and reverse transcriptase (Lown et al., 1986).

The numbering system used is the genomic numbering system of pBR-322 DNA (Maniatis et al., 1982). Experimental protocols for the footprinting experiments and the synthesis of MnT4MPyP were as previously described (Ward et al., 1987; Raner et al., 1988).

Briefly, all reactions were carried out in 50 mM Tris-HCl buffer at pH 7.5 for 20 min at 37 °C. The final DNA concentration in base pairs in each of the 14 reactions was 194  $\mu$ M (193  $\mu$ M sonicated calf thymus DNA and  $\sim$ 1  $\mu$ M labeled fragment). Two control reactions were carried out in the absence of netropsin by equilibrating the porphyrin and DNA for 30 min in a total volume of 6  $\mu$ L followed by the addition of 2  $\mu$ L of a 4 mM solution of freshly prepared oxone,  $\text{KHSO}_5$ , in buffer. The 12 reactions involving netropsin were carried out in an identical manner by incubating the drug and the porphyrin with DNA for 30 min in 6  $\mu$ L followed by the addition of 2  $\mu$ L of the activating agent. The final total concentration of porphyrin in all experiments was 1.3  $\mu$ M. Final total concentrations of netropsin employed in the various experiments were as follows ( $\mu$ M): 1.09, 1.50, 2.08, 2.88, 3.99, 5.52, 7.64, 10.6, 14.6, 20.3, 27.0, and 38.8. After termination of the digest, the reaction products were separated in a 12% denaturing polyacrylamide gel with a thermostated field gradient electrophoresis device developed in-house. The resulting autoradiogram, Figure 1, was scanned with a linear scanning microdensitometer to yield band cross-sectional areas ( $a_i$  = band area for site  $i$ ) directly proportional to oligonucleotide concentrations (Dabrowiak et al., 1986). Single-nucleotide resolution was obtained at position 45-110 with lower resolution at positions above 110. Establishment of sequence was as earlier described (Lown et al., 1986).

Careful inspection of the ladder of bands produced by porphyrin cleavage relative to those produced by DNase I cleavage revealed that the shortest porphyrin oligomer, a 13-mer, migrated more slowly, by  $\sim$ 1 nucleotide, than the corresponding DNase I oligomer. The longer oligomers from both sources showed a 1:1 correspondence in electrophoretic mobility. Since the ladder of porphyrin-produced bands is not complete, as is that produced by DNase I, the lack of correspondence of the shorter oligomers went unnoticed in earlier work involving the porphyrin (Ward et al., 1986, 1987), leading to an error in sequence assignment for the porphyrin cleavage in the region 45-51. The corrected porphyrin cleavage sites, its binding sites, and those of the drug are shown on the sequence of the fragment in Figure 2.

The 5'-terminal sequence 5'-ATTAAA-3' at positions 38-33 would be expected to bind both drug and porphyrin. However, due to their short lengths, these oligomers migrated from the end of the gel into the buffer well, and thus no direct infor-

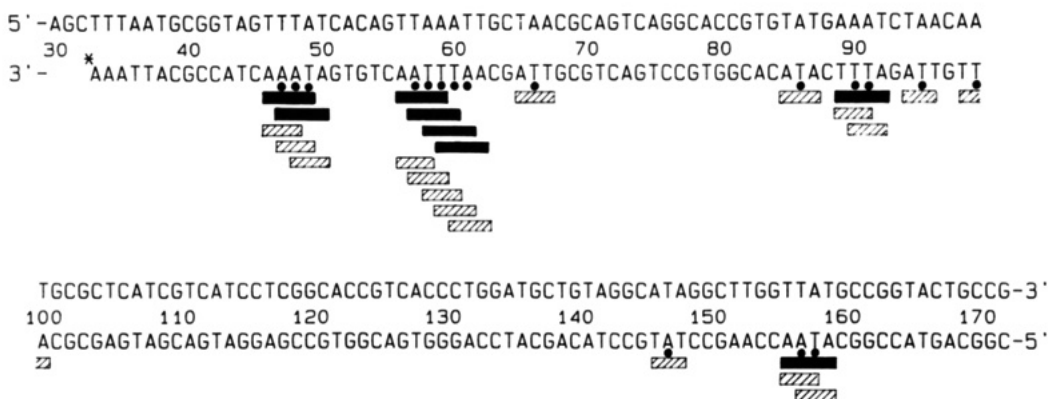


FIGURE 2: Sequence of the *HindIII*/*NciI* 139 base pair restriction fragment of pBR-322 DNA. The asterisk denotes the position of the radiolabel. Porphyrin cleavage site (●); porphyrin binding site (hatched bar); netropsin binding site (solid bar).

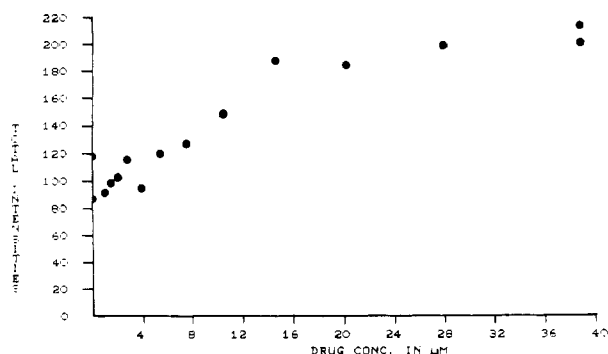


FIGURE 3: Total amount of cleavage on the 139-mer in arbitrary units plotted versus total netropsin concentration.

mation on netropsin affinity for this sequence could be obtained.

The porphyrin cleavage products appeared to be "clean", and only one band representing each oligomer was detected. However, a minor band migrating at position  $\sim 62$  did not appear to be part of the porphyrin-produced ladder. Since it also appeared on other autoradiograms involving porphyrin cleavage of the 139-mer but at a slightly different position, it was ignored in the present analysis. The autoradiogram showed 90 and 91 to be two distinct bands but the densitometer summed the band area for both sites under a single peak indexed as 91. Sites 157 and 158, in an unresolved portion of the autoradiogram, were indexed as a single site, 157.

In order to smooth the data for intensity as a function of netropsin concentration, the sum of all of the band areas except for the full-length band was obtained for each digest. Plotting this sum against the total concentration of netropsin present in the system showed that addition of drug led to an increase in the amount of cleavage on the 139-mer (Figure 3). On least-squares fitting the summed areas to polynomial functions of  $D_t$ , the total netropsin concentration, we found the quadratic

$$A(D_t) = 92.06 + (6.441 \times 10^6)D_t - (9.075 \times 10^{10})D_t^2 \quad (1)$$

fit significantly better than the linear function. Cubic and higher polynomials gave no improvement in fit. To smooth the data and correct for loading errors and differences in digest time, each observed site area,  $a_i$ , was multiplied by the ratio of  $A$  determined from eq 1 to the experimentally determined value of  $A$  for the same value of  $D_t$ . The correction factors obtained in this manner were in the range from 0.9 to 1.1.

Inspection of the control band of uncut fragment on the autoradiogram revealed that a small amount of radioactive material migrated in the direction of electrophoresis. This "bleeding" effect was subtracted from the data by scanning the control lane and determining the appropriate area correction for a particular band on the autoradiogram. This correction, which was greatest for the site nearest the origin band site (157), was less than 10% of the total area associated with the cleavage at this site.

## RESULTS

From the experiments for zero drug concentration, one can immediately identify the preferred porphyrin binding regions to be 46–50, 56–62, 65–67, 85–87, 89–92, 94–96, 98–100, 146–149, and 156–159. These correspond to sequences of at least three contiguous A or T bases (Figures 1 and 2). The cleavage pattern for a site can be explained if the bound porphyrin cuts in the middle of the A-T trimer to which it is bound. This is true for isolated trimers as well as for trimers which are part of longer A-T sequences.

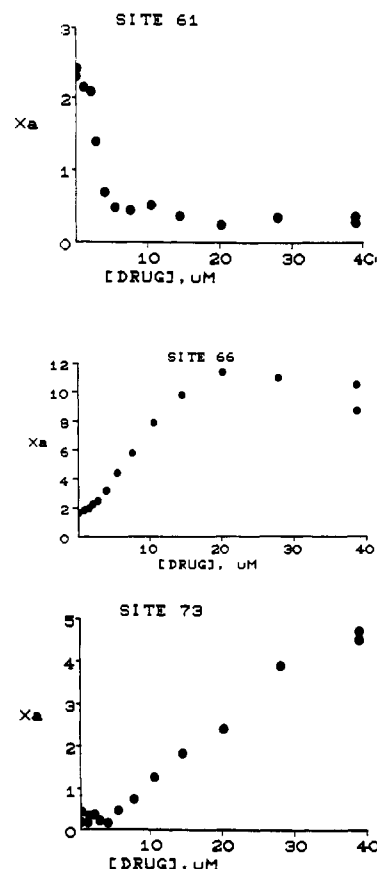


FIGURE 4: Footprinting plots of corrected autoradiographic spot intensities versus total netropsin concentration. The site numbers refer to the sequence in Figure 2.

As drug is added to the system, three different types of footprinting plots are observed, as illustrated in Figure 4. Strong netropsin sites, all of type  $(A \cdot T)_4$ , show rapid decreases in intensity with increased drug concentration, Figure 4, site 61. The observed decrease represents the direct effect of bound drug, preventing porphyrin from binding at these sites: the classic footprinting phenomenon. The positions for which this occurs are 46–50, 56–62, 89–92, and 146–149. Sites of type  $(A \cdot T)_3$ , 66, 86, 95, 99, and 147, initially show enhanced intensity with added drug as shown in Figure 4, site 66. However, since these sites are weak netropsin binding sites, they eventually exhibit inhibition of higher drug concentrations. Enhancements also occur for weaker porphyrin binding sites, but only for  $D_t$  in the range from 7.64 to 38.8  $\mu M$  (see Figure 4, site 73). These sites are all of the type  $(A \cdot T)(G \cdot C)_2$  or  $(A \cdot T)_2(G \cdot C)$ .

In order to consider the change in the porphyrin–DNA equilibrium as netropsin was added to the system, the amount of increase in cleavage at the centers of the isolated  $(A \cdot T)_3$  sites (66, 86, 95, 99, and 147) as a function of netropsin concentration was calculated. For each site we fit the first nine intensities (for  $D_t \leq 3.99 \mu M$ ) to quadratic functions of drug concentration and divided the slope at  $D_t = 0$  by the intensity at  $D_t = 0$  to obtain the relative enhancement. The results (all times  $10^{-5}$ ) were  $1.39 \pm 0.59$ ,  $0.68 \pm 0.47$ ,  $0.79 \pm 0.70$ ,  $3.31 \pm 1.28$ , and  $1.53 \pm 0.40$ . Probable errors were calculated according to Appendix I found in the supplementary material.

Inspection of the data revealed that in the concentration range  $0 \leq D_t \leq 10.6 \mu M$  only the strong drug sites on the 139-mer were accepting netropsin. In calculating binding constants for the strong sites, the intensity data associated with 15 porphyrin cleavage sites, shown as dots in Figure 2, were

used in the analysis. (Data for sites 90 and 91 were taken together, as were data for 157 and 158.) Ten of these sites, 46–50, 56–62, and 89–92, were located within strong netropsin sites and behaved like site 61, Figure 4. The other five porphyrin sites, all isolated A-T trimers (66, 86, 95, 99, and 147), were outside of strong netropsin sites, e.g., site 66, Figure 4. No weak porphyrin binding sites, e.g., site 73, Figure 4, were used in the analysis. The eight different drug concentrations plus two digests carried out in the absence of netropsin give rise to 150 intensities (concentrations) to be fit by the model.

#### ANALYSIS AND MODEL

**Site Exclusions.** We consider how a drug molecule, which is four nucleotides long, can exclude a porphyrin from its trinucleotide binding site. For the isolated drug sites of type (A·T)<sub>4</sub> at positions 89–92 and 156–159 (Figure 2), occupancy by a netropsin molecule excludes both possible modes of porphyrin binding to the tetranucleotide sequence. If a netropsin site is a contiguous set of base pairs indexed by  $(i, i+1, i+2, i+3)$ , where  $i$  is the nucleotide location closest to the label, porphyrin binding at both  $(i, i+1, i+2)$  and  $(i+1, i+2, i+3)$  is excluded by drug. If the drug binding constant for binding to  $(i, i+1, i+2, i+3)$  is denoted by  $K_i$

$$K_i = c_i/D_o c_f \quad (2)$$

in which  $c_i$  is the concentration of sites  $i$  at which drug is bound,  $c_f$  is the concentration of free sites  $i$ , and  $D_o$  is the concentration of free drug. The fraction of site  $i$  which is occupied by drug,  $\nu_i$ , is then given by

$$\nu_i = K_i D_o / (1 + K_i D_o) \quad (3)$$

Since binding of drug to an isolated tetramer blocks both modes of porphyrin binding to the tetramer, the fraction of a porphyrin binding site which is free to be occupied by porphyrin,  $f_i$ , is the same for both  $i$  and  $i+1$ , i.e.

$$f_i = f_{i+1} = 1 - \frac{K_i D_o}{1 + K_i D_o} \quad (4)$$

The situation with the A-T pentamer at positions 46–50, Figure 2, is similar except that drug may occupy two different positions within the sequence, either of which excludes the binding of the porphyrin to all three of its binding sites within the segment. The probability that drug covers the sites from  $i$  to  $i+3$  is  $K_i D_o (1 + K_i D_o + K_{i+1} D_o)^{-1}$ , and the probability that drug covers the sites from  $i+1$  to  $i+4$  is  $K_{i+1} D_o (1 + K_i D_o + K_{i+1} D_o)^{-1}$ . Since either situation will prevent the binding of porphyrin

$$f_i = f_{i+1} = f_{i+2} = 1 - \frac{K_i D_o (1 + K_i D_o + K_{i+1} D_o)^{-1} + K_{i+1} D_o (1 + K_i D_o + K_{i+1} D_o)^{-1}}{1 + K_i D_o + K_{i+1} D_o} = 1 / (1 + K_i D_o + K_{i+1} D_o) \quad (5)$$

For the A-T heptamer, located at positions 56–62, Figure 2, the situation is more complicated. The size of netropsin on DNA is ~4 base pairs and the size of porphyrin ~3 base pairs, so drug binding to  $(i+1, i+2, i+3, i+4)$  or  $(i+2, i+3, i+4, i+5)$  will exclude porphyrin binding to any of its five possible binding sites within the sequence ( $i = 56$  here). Since the probability that no drug is bound to the heptamer is  $(1 + K_i D_o + K_{i+1} D_o + K_{i+2} D_o + K_{i+3} D_o)^{-1}$ , the fraction of the three interior binding sites within the heptamer which can bind porphyrin is

$$f_{i+1} = f_{i+2} = f_{i+3} = (1 + D_o \sum_{j=0}^3 K_{i+j})^{-1} \quad (6)$$

However, it is theoretically possible to have the porphyrin and

the drug simultaneously occupy the heptamer if the drug is bound to  $(i, i+1, i+2, i+3)$  while the porphyrin occupies  $(i+4, i+5, i+6)$ . An equivalent situation exists for porphyrin occupation of the lowest numbered sites within the heptamer. Although electrostatic effects would discourage simultaneous occupations on the same DNA restriction fragment (both the porphyrin and the drug are cations), it was considered a possibility in our analysis in order not to introduce additional parameters to describe the anticooperativity. The fraction of the first end site which is free of drug is

$$f_i = 1 - D_o \sum_{j=0}^2 K_{i+j} (1 + D_o \sum_{j=0}^3 K_{i+j})^{-1} = D_o K_{i+3} (1 + D_o \sum_{j=0}^3 K_{i+j})^{-1} \quad (7)$$

Similarly

$$f_{i+5} = D_o K_i (1 + D_o \sum_{j=0}^3 K_{i+j})^{-1} \quad (8)$$

There are no A-T sequences of length greater than seven on the *HindIII/NciI* restriction fragment, and the complications just discussed do not occur for A-T segments of smaller length.

**Enhancements.** In quantitative experiments involving DNase I and netropsin (Ward et al., 1988a,b) addition of drug to the system did not cause a change in the total amount of cleavage taking place on the 139-mer. This showed that the equilibrium between the enzyme and DNA was not disturbed during the footprinting titration and that the enhancements found in nonbinding regions of the polymer canceled the inhibitions occurring at binding sites. However, the total amount of cleavage on the fragment is sensitive to the nature of the carrier DNA. If, for example, the carrier is poly(dAdT)·poly(dAdT), which possesses many more netropsin binding sites than the 139-mer, addition of drug causes the enzyme to be displaced from the carrier to the fragment. This gives rise to an increase in total cleavage similar to that shown in Figure 3 for MnT4MPyP (Ward and Dabrowiak, unpublished).

The porphyrin cleaves with much higher specificity than DNase I. Furthermore, a large fraction of its binding sites are also drug binding sites. If the ratios of drug-blocked porphyrin sites to free porphyrin sites on the carrier and the fragment were the same, total cleavage on the fragment would remain constant as drug is added to the system. As is shown in Figure 3, this is clearly not the case. Since an increase in cleavage is observed, drug must be displacing porphyrin from the carrier to the fragment as the titration proceeds. This can be easily confirmed by determining the ratio of isolated trinucleotide sites of type (A·T)<sub>3</sub> to longer contiguous tracts of A and T on both the carrier and the fragment. While an isolated trimer can bind only porphyrin, the latter type of site can bind both the drug and MnT4MPyP. From Figure 2, the ratio between the numbers of these two types of site is ~1 for the fragment while for calf thymus DNA it can be estimated by assuming this carrier is a random arrangement of A-T and G-C (see Appendix 2 in the supplementary material), as ~0.67. Thus, addition of drug to the system will result in a release of porphyrin from the carrier, ultimately causing increased cleavage on the fragment. This mechanism implies that the change in the porphyrin–DNA equilibrium can be directly monitored via the cleavage increases at sites of type (A·T)<sub>3</sub> on the fragment and that the enhancement due to the effect should be the same at all netropsin binding sites.

The actual enhancements for sites of type (A·T)<sub>3</sub> on the fragment (initial slope divided by intensity for zero drug), given

in the previous section, are in fact the same within the estimated errors (average value =  $1.54 \pm 0.63$ ). The probable error in each is as large or larger than the variance, 0.63. Further, these enhancements are twice that which should result from drug displacement of porphyrin from only the primary netropsin sites on the fragment. The enhancement due to such displacement is calculable from the number of binding sites on the fragment. Finally, a simple redistribution mechanism, which was invoked for DNase I (Ward et al., 1988b), would give no change in total cleavage with added drug, contradicting eq 1.

**Reporting of Site Occupancy by the Cleavage Agent.** In the quantitative footprinting experiment, the change in the amount of cleavage at a particular site is used to measure the fraction of that site which is occupied by a drug molecule,  $\nu_i$ . In studies involving DNase I, it is assumed that the cleavage rate at site  $i$  is proportional to  $1 - \nu_i$  or  $f_i$ , calculated by equations like 4–8. This assumption yielded reasonable binding constants for netropsin, *lac*, and *trp* repressors toward their interaction sequences (Brenowitz et al., 1986a,b; Seneor, 1986; Carey, 1988; Ward et al., 1988a).

DNase I, unlike MnT4MPyP, binds and cleaves at nearly every nucleotide position, so that it acts as if it "sees" a series of contiguous binding sites. If the barrier height between sites is less than  $kT$ , it is possible for the enzyme to easily transit in a one-dimensional diffusional process between sites on the DNA lattice (Winter & von Hippel, 1981). Effectively, it is not bound to a specific site but rather to the entire fragment. However, if the probe specificity is high, as is the case with MnT4MPyP, the barrier height for transiting from a specific site, e.g., an isolated trimer of type (A·T)<sub>3</sub>, to another site which binds porphyrin is likely to be high. Then it is appropriate to consider that there is a classic equilibrium between unbound cleavage agent and agent bound to a site. In this case, the cleavage at a particular site will *not* be proportional to  $f_i$ , as can be shown with a simple example.

Let  $K_i$  and  $Q_i$  represent the binding constants for drug and probe at a site. Let  $c$  be the total concentration of such sites,  $P_t$  the total probe concentration, and  $D_b$  and  $P_b$  the concentration of these sites at which drug and probe, respectively, are bound. The cutting rate is proportional to  $P_b$  and  $\nu_i = D_b/c$ . The equilibrium expression

$$Q_i = \frac{P_b}{(P_t - P_b)(c - D_b - P_b)} \quad (9)$$

is solved to give

$$P_b = \frac{1}{2}cf_i + \frac{1}{2}P_t + (2Q_i)^{-1} - \left[ \left( \frac{1}{2}cf_i + \frac{1}{2}P_t + \frac{1}{2Q_i} \right)^2 - cP_f f_i \right]^{1/2}$$

which shows that  $P_b$  is not proportional to  $\nu_i$ . Expanding the square root

$$P_b = cf_i - \frac{cf_i}{P_t Q_i} - \frac{(Q_i^{-1} - cf_i)^3}{4P_t^2} + \dots \quad (10)$$

Thus,  $P_b$  will be proportional to  $f_i$  if  $P_t$  is large compared to  $c$  and  $Q_i^{-1}$ . This means that, for the footprinting experiment to report the fraction of binding site unoccupied by drug, the probe binding constant and the amount of probe must be large enough to saturate the site with probe. For the experiments reported here,  $c$  and  $P_t$  are  $\sim 50 \mu\text{M}$  and  $1.3 \mu\text{M}$ , respectively. On the basis of studies involving related porphyrins, the binding constant of Mn4MPyP toward calf thymus DNA can be es-

timated to be  $\sim 10^7 \text{ M}^{-1}$  (Geacintov, 1987). Thus, for these experiments, the cutting rate should not be proportional to  $\nu_i$ .

We attempted at first to fit the present data using the same model employed for analyzing the DNase I experiments, but the fit was less good than in previous work (Ward et al., 1988a). More important, the values found for the drug binding constants were all 1–2 orders of magnitude lower than the values found previously. It is now clear that this is due to the incorrect assumption that the observed cutting rates by the porphyrin directly report the fraction of a site which is occupied by drug. It is clear from eq 10 that this is not so.

**Role of the Carrier DNA.** The concentration of bound probe and the concentration of bound drug are determined by equilibria like eq 9. When carrier DNA is present in excess, equilibria with carrier sites are more important than equilibria with sites on the labeled restriction fragment. The equilibria with carrier sites then determine free drug and free porphyrin concentrations ( $D_f$  and  $P_f$ ) which, through the equilibria with fragment sites, determine the bound drug and bound porphyrin concentrations. For example, the right side of eq 9 would be written as  $P_b/[P_f(c - D_b - P_b)]$  and the drug binding equilibrium as

$$K_i = \frac{D_b}{D_f(c - D_b - P_b)} \quad (11)$$

From a model for the carrier, one can determine  $P_f$  and  $D_f$  by considering similar equilibria.

The increase in cutting rate at A-T trimers on the labeled fragment, as drug is added, is caused by the drug displacing the porphyrin from its carrier binding sites to solution. Total cleavage on the 139-mer  $I_t(r_i)$  should increase with total drug concentration initially and level off subsequently, when all carrier sites which can bind *both* drug and probe become saturated with drug. This is reflected in eq 1 by the negative sign of the quadratic term, which leads to a maximum value of  $A$  of 206.3. When  $I_t$  levels off, the free probe concentration becomes equal to the total probe concentration minus the concentration of probe bound to sites which can bind probe but not drug (A-T trimers). The ratio of the amount of porphyrin bound to fragment when no drug is present to the amount bound when drug saturates all sites on the carrier is 206.3/92.06 or about 2.3.

The carrier, calf thymus DNA, is considered to consist of a random arrangement of two kinds of sites, A-T bases and G-C bases, with a given fraction,  $p$ , being A-T bases. We choose  $p = 0.6$  (Marmur & Doty, 1962) and use probability theory to calculate the numbers of various kinds of drug and porphyrin sites present in calf thymus DNA: isolated A-T trimers, isolated A-T tetramers, etc. (Appendix 2). Given values for drug and porphyrin binding constants, free drug and free porphyrin concentrations can be calculated for any total drug concentration. Note that the carrier serves as a buffer for both drug and porphyrin, i.e., the binding equilibria for the carrier determine the free porphyrin and free drug concentrations, which in turn determine the amounts of drug and porphyrin bound to sites on the fragment.

Our model for the carrier shows that a plot of free porphyrin concentration  $P_f$  vs total drug concentration  $D_t$  is initially linear, with positive slope, but the slope decreases afterward and the free porphyrin concentration levels off. This is because porphyrin continues to bind to A-T trimers, while drug cannot bind, while other porphyrin sites become saturated with drug. The free drug concentration  $D_f$  also increases with total drug concentration, slowly at first and then linearly, after drug binding sites on the carrier are saturated. Figure 5 shows

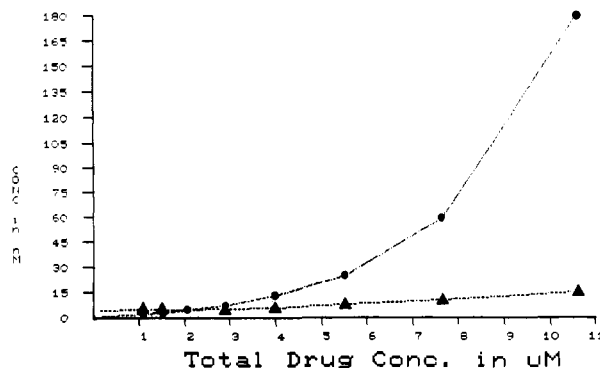


FIGURE 5: Plot showing the free netropsin concentration (●) and free porphyrin concentration (▲) as a function of the total netropsin concentration.  $K_p = 1.1 \times 10^7 \text{ M}^{-1}$ ;  $K_d = 3.5 \times 10^7 \text{ M}^{-1}$ ;  $K_w = 1.0 \times 10^6 \text{ M}^{-1}$ .

calculated free porphyrin and free drug concentrations for the range of total drug concentrations used in the analysis. The asymptotic behaviors (leveling off of  $P_f$ , linear dependence of  $D_f$  on  $D_t$ ) are not shown for this range of  $D_t$ .

The cutting rate at a site will be assumed to be proportional to the concentration of porphyrin at that site, as calculated from the appropriate competitive binding equilibrium expression and the free drug and free porphyrin concentrations  $D_f$  and  $P_f$ . These concentrations, calculated by considering equilibria with carrier sites, detailed in Appendix 2, depend on the values of the drug and porphyrin binding constants to carrier sites. Like the binding constants to fragment sites, the binding constants to carrier sites will be determined to give the best fit of calculated to experimental footprinting data.

**Cutting Rates.** For an isolated A-T trimer, the cutting rate is proportional to  $K_p P_f (1 + K_p P_f)^{-1}$ . An A-T tetramer on the fragment can bind either drug (binding constant  $K_i$ ) or porphyrin (in two ways), so that the cutting rate at either interior position is proportional to

$$\chi_p = K_p P_f (1 + 2K_p P_f + K_i D_f)^{-1} \quad (12)$$

There can be no cutting at the end positions according to our model. An A-T pentamer can bind either drug or porphyrin, the former in two ways and the latter in three ways, so that the cutting rate at any of the three interior positions is proportional to

$$\chi_p = K_p P_f (1 + 3K_p P_f + K_i D_f + K_{i+1} D_f)^{-1} \quad (13)$$

Here,  $K_i$  and  $K_{i+1}$  are binding constants for the two overlapped drug binding sites. The constants for the individual sites cannot be determined according to eq 13.

The heptamer corresponding to A-T's at positions  $i$  to  $i + 6$  ( $i = 56$ ) can bind one or two porphyrins, or a drug molecule and a porphyrin, and cutting can take place at positions  $i + 1$  to  $i + 5$ . Considering all the situations, we find the cutting rate at  $i + 1$  to be proportional to

$$\chi_p = [K_p P_f + 4(K_p P_f)^2 + K_p P_f K_{i+4} D_f] / [1 + 5K_p P_f + 6(K_p P_f)^2 + (K_{i+1} + K_{i+2} + K_{i+3} + K_{i+4}) D_f + K_p P_f (K_{i+1} + K_{i+4}) D_f] \quad (14)$$

where  $K_{i+1}$  to  $K_{i+4}$  are the four drug binding equilibrium constants associated with drug binding to the heptamer. For the cutting rate at  $i + 5$ ,  $K_{i+4}$  and  $K_{i+1}$  are interchanged in eq 14. Cutting at  $i + 2$  is proportional to

$$\chi_c = [K_p P_f + 2(K_p P_f)^2] / [1 + 5K_p P_f + 6(K_p P_f)^2 + (K_{i+1} + K_{i+2} + K_{i+3} + K_{i+4}) D_f + K_p P_f (K_{i+1} + K_{i+4}) D_f] \quad (15)$$

and the same expression describes cutting at  $i + 4$ . For cutting at  $i + 3$ , the porphyrin must occupy positions  $i + 2$ ,  $i + 3$ , and  $i + 4$  and no other porphyrin or drug can then bind, so the rate is proportional to

$$\chi_d = (K_p P_f) / [1 + 5K_p P_f + 6(K_p P_f)^2 + (K_{i+1} + K_{i+2} + K_{i+3} + K_{i+4}) D_f + K_p P_f (K_{i+1} + K_{i+4}) D_f] \quad (16)$$

According to eq 14–16, the individual values of  $K_{i+2}$  and  $K_{i+3}$  cannot be determined, but just their sum.

On first attempting to fit experimental intensities with this model, we found that there were large discrepancies between the theoretical and experimental points for the highest drug concentration used,  $10.58 \mu\text{M}$ . With an effective concentration of primary sites of type (A-T)<sub>4</sub> present in the system of  $\sim 10^{-5} \text{ M}$  (see Appendix 2), the carrier would be saturated by drug before  $D_t = 10.58 \mu\text{M}$ , causing  $D_f$  to increase rapidly with  $D_t$ . This would give a sharp decrease in fragment cutting rates with  $D_t$ , which was not experimentally observed. Thus, there are other (weaker) drug binding sites on the carrier which keep the free drug concentration low at higher values of total drug concentration. Previous footprinting studies by us (Ward et al., 1988a) have shown that these weak sites are probably tetramers including one G or C. To take them into account, we assume that, in addition to strong binding sites, the carrier possesses weak drug binding sites at a concentration twice that of A-T trimers, which are one kind of weak netropsin site. The netropsin binding constant for these weak sites,  $K_w$ , is at least 2 orders of magnitude lower than the binding constants for the strong sites ( $10^7$ – $10^8 \text{ M}^{-1}$ ). The precise value of  $K_w$ , as might be expected, does not significantly affect the determined values of binding constants for the strong sites; it only helps improve the fit between calculated and experimental intensities at a few points (for the highest drug concentration) in the entire data set.

#### CALCULATION OF BINDING CONSTANTS

Assuming values for  $K_p$ ,  $K_w$ , and  $K_d$  and using the statistically determined concentrations of A-T trimers, tetramers, ..., octamers on the carrier, and weak drug sites on the restriction fragment, we can calculate free drug and free porphyrin concentrations for each known total drug concentration by solving the simultaneous equations for carrier equilibrium (Appendix 2). The resulting values for free porphyrin and free drug concentrations,  $P_f$  and  $D_f$ , are used with values for the  $K_i$  to compute the amount of porphyrin bound at each site on the labeled fragment, and hence the footprinting autoradiographic spot intensities for comparison with experimental intensities. The binding constants for drug molecules on fragment sites are then chosen to minimize the sum of the squared deviations between experimental and calculated spot intensities.

Initially, the value of the porphyrin binding constant to sites of type (A-T)<sub>3</sub>,  $K_p$ , was chosen as  $1 \times 10^7 \text{ M}^{-1}$ . Various values for  $K_d$  (drug binding constant to carrier) were used, as discussed below. In our previous calculation (Ward et al., 1988a), we assumed a concentration of drug sites on the carrier of  $190 \mu\text{M}$  and determined a binding constant for these sites of  $1 \times 10^6 \text{ M}^{-1}$ , which represents an average between the constants for strong sites and others. Since the strong-site concentration for the present calculation is  $\sim 17 \mu\text{M}$  (see Appendix 2), the value of  $K_d$  should be about  $1.1 \times 10^7 \text{ M}^{-1}$ . As pointed out previously, it is the product of  $K_d$  and the site concentration that is important. The total porphyrin concentration  $P_t$ , measured optically, was  $1.3 \mu\text{M}$  in all the experiments considered here, while  $D_t$ , the total netropsin concentration, varied from 0 to about  $10 \mu\text{M}$ .

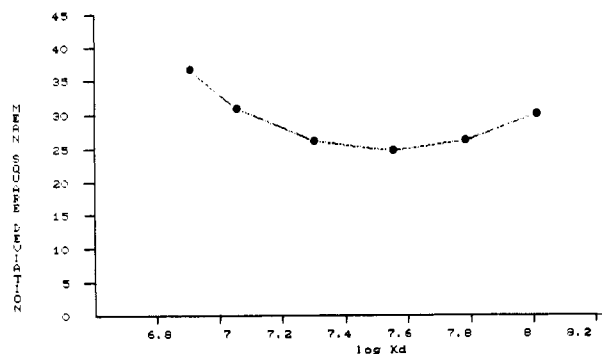


FIGURE 6: Plot showing the variation in the value of the mean-square deviation,  $D$ , as a function of the binding constant of netropsin for sites on the carrier DNA.

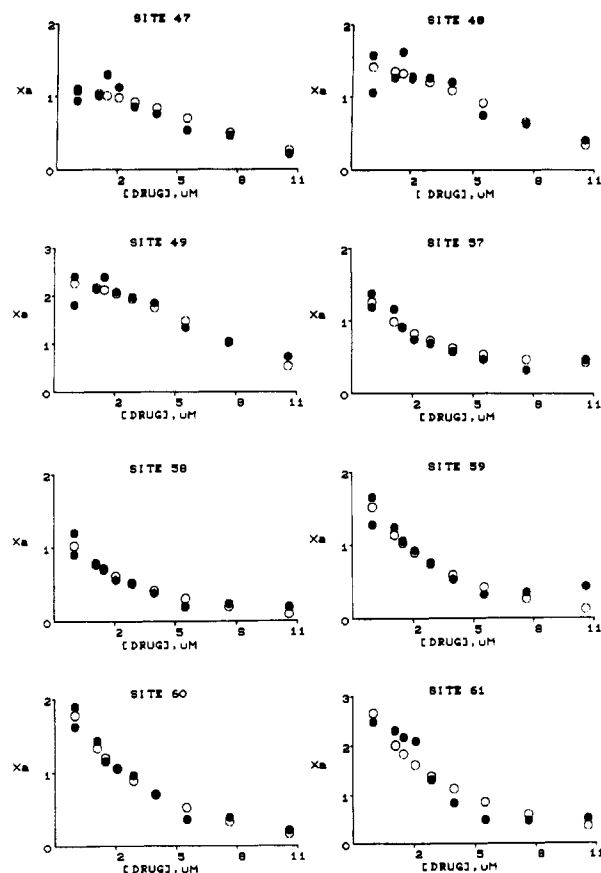


FIGURE 7: Experimental (●) and calculated (○) footprinting plots for various binding and enhancement sites on the 139-mer.  $K_p = 1 \times 10^7 \text{ M}^{-1}$ ;  $K_d = 3.5 \times 10^7 \text{ M}^{-1}$ ;  $K_w = 1.0 \times 10^6 \text{ M}^{-1}$ .

The site binding constants for drug on the fragment are determined by searching, using the simplex search algorithm (Fletcher, 1980), for the set which minimizes the sum of the squared deviations between the experimental and calculated spot intensities. For any set of values for  $K_d$ ,  $K_p$ , and  $K_w$  the algorithm converges properly to yield the set of  $K_i$  which minimizes:

$$D = \sum_i \sum_j (I_{ij} - \bar{I}_{ij})^2 \quad (17)$$

where  $I_{ij}$  is the experimental intensity for site  $i$  at the  $j$ th total drug concentration and  $\bar{I}_{ij}$  is the corresponding calculated value. The resulting mean-square deviation,  $D$ , is smaller than what we obtained with the earlier study involving DNase I as a footprinting probe (Ward et al., 1988a). Due to the sizes of the porphyrin and the drug when bound to DNA, the cutting-rate expressions do not allow the determination of all  $K_i$ , but only  $K_{46} + K_{47}$ ,  $K_{56}$ ,  $K_{57} + K_{58}$ ,  $K_{59}$ ,  $K_{89}$ , and  $K_{156}$ .

Table I: Netropsin Binding Constants ( $\times 10^{-7} \text{ M}$ )<sup>a</sup>

nucleotide position <sup>b</sup>	sequence of site	MnT4MPyP	DNase I <sup>c</sup>	
46 + 47	TTTAT AAATA	7.8	9	8 <sup>d</sup>
56	TTAA AATT	0.4	0.3	0.2 <sup>d</sup>
57 + 58	TAAAT ATTTA	26	18	20 <sup>d</sup>
59	AATT TTAA	1.4	13	7 <sup>d</sup>
89	AAAT TTTA	5.3	14	10 <sup>d</sup>
156	TTAT AATA	2.1	8	1 <sup>d</sup>

<sup>a</sup> Values were determined with  $K_d = 3.5 \times 10^7 \text{ M}^{-1}$ ,  $K_p = 1.0 \times 10^7 \text{ M}^{-1}$ , and  $K_w = 1.0 \times 10^6 \text{ M}^{-1}$ . <sup>b</sup> The position of the lowest numbered nucleotide of the tetramer binding site is given, see Figure 2. <sup>c</sup> Data from Ward et al. (1988a). <sup>d</sup> Carrier-free experiment.

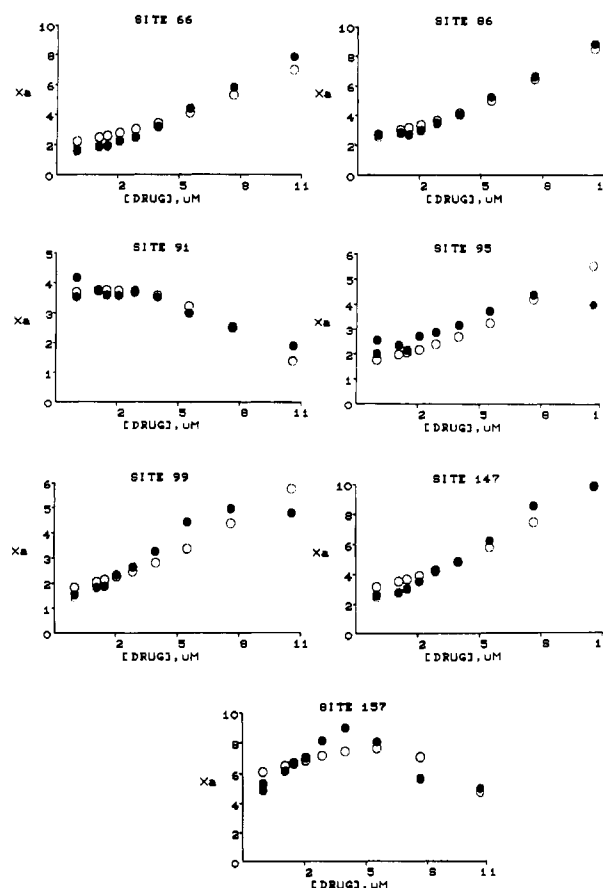


FIGURE 8: See caption for Figure 7.

Figure 6 is a plot of the lowest value of  $D$  found for various choices of  $K_d$ , the netropsin binding constant to the carrier. It is seen that there is a clear minimum for  $K_d \sim 3.5 \times 10^7 \text{ M}^{-1}$ . The value of  $K_d$  is thus determined, like the values of  $K_i$ , by minimization of  $D$  in eq 17. In Table I, we give the  $K_i$  values corresponding to this minimum and compare them with the values found by analysis of DNase I footprinting data. The experimental intensities are compared with the calculated ones for the "best fit" in Figures 7 and 8 (Ward et al., 1988a).

As is evident from Table I, the netropsin binding constants obtained with DNase I and MnT4MPyP are in the same rank order and are in generally good agreement with regard to magnitude. The site with the lowest binding constant, 56, contains the sequence 5'-TA-3' which is expected to produce a distortion in the minor groove of DNA (Calladine, 1982). Although further study will be necessary, this distortion likely produces less than optimum drug-DNA contacts, leading to a decrease in the binding constant of netropsin. Agreement between the DNase I and MnT4MPyP data appears poorest for site 59. Since this site is in a heavily overlapped region



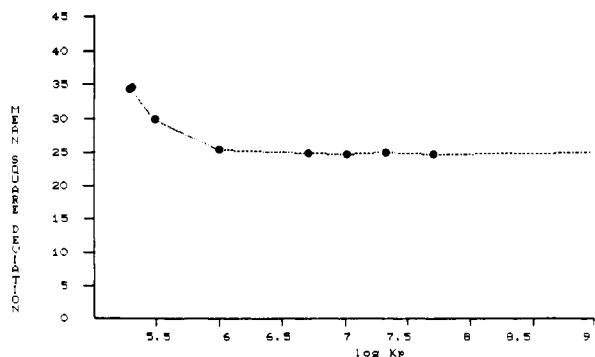


FIGURE 9: Plot showing the mean-square deviation,  $D$ , as a function of the porphyrin binding constant,  $K_p$ , to its DNA interaction sites.  $K_d = 3.5 \times 10^7 \text{ M}^{-1}$ ;  $K_w = 1.0 \times 10^6 \text{ M}^{-1}$ .

of the polymer and the porphyrin yields fewer footprinting plots than the enzyme which can be used to determine  $K_i$ , the precision of this value is lower than that associated with DNase I.

We also investigated the sensitivity of the determined values of  $K_i$  for netropsin to the value of  $K_p$ , the porphyrin binding constant. Keeping  $K_d = 3.5 \times 10^7 \text{ M}^{-1}$ , we assumed different values of  $K_p$  and carried out the minimization of  $D$  with respect to the  $K_i$ . As is evident from Figure 9, the value of the mean-square deviation  $D$  (eq 17) is independent of  $K_p$  for  $K_p$  in the range  $10^6$ – $10^9 \text{ M}^{-1}$ . For this range of  $K_p$  the determined values of  $K_i$  were the same as those given in Table I. This is because, as long as  $K_p$  is large enough to make  $P_f$  small compared to  $P_i$ , the carrier–netropsin equilibrium expression

$$P_i = P_f + \frac{c_3 K_p P_f}{1 + K_p P_f} + \frac{2C_4 K_p P_f}{1 + 2K_p P_f + K_d D_f} + \dots$$

(Appendix 2, eq 11) involves only the product  $K_p P_f$ , so doubling the assumed value of  $K_p$  simply divides all of the calculated values of  $P_f$  by 2. The same  $K_p$  is used for the fragment as for the carrier, and only  $K_p P_f$  enters eq 12–16. Thus, if  $K_p > \sim 10^6 \text{ M}^{-1}$ , it is unimportant to know its exact value in calculating valid binding constants for the drug bound to its interaction sequences.

## CONCLUSIONS

In this paper we have examined the ability of the AT-specific cleaving agent MnT4MPyP to report valid binding information for netropsin bound to a 139 base pair restriction fragment of pBR-322 DNA. The reporting of site occupancy by the porphyrin is different from that of DNase I. The behavior of the latter may be understood by considering that DNase I “sees” a closely spaced collection of sites on DNA with comparable binding constants. The potential surface involves closely spaced minima, so the barrier to movement from one site to its neighbor cannot be very large and the enzyme can be thought of as being bound to the fragment as a whole rather than to a specific site on the fragment. On the other hand, the porphyrin complex “sees” a few well-separated minima, so that it is appropriate to consider binding equilibria for individual sites on the fragment. As we have shown, analysis of the porphyrin data using the model developed for DNase I leads to equilibrium constants for netropsin which are several orders of magnitude lower than those previously determined (Ward et al., 1988a). The redistribution model employed for DNase I is also incapable of explaining the increase in the total amount of cleavage on the fragment with added drug, or the magnitude of the drug-induced enhancement in cutting rate at sites where netropsin cannot bind. These are explained naturally in the model presented above, which considers

competitive binding of drug and porphyrin at specific sites on both the fragment and carrier DNA present. Analysis according to this model also yields site-specific binding constants for netropsin in good agreement with previously determined values.

While the high specificity of MnT4MPyP prevents it from being a “broad spectrum” footprinting probe useful for studying ligands of unknown specificity, it can be used to measure binding constants for drugs with affinities for AT sites. In this respect it is similar to the AT-specific compound Cu(o-phen)<sub>2</sub> which has been used in footprinting experiments involving netropsin and the duplex d(CGCGAATTCGCG)<sub>2</sub> (Kuwabara et al., 1986). From the present study and earlier published experimental (Ward et al., 1988a) and theoretical work (Goodisman & Dabrowiak, 1985), it is clear that the detailed mechanism by which the probe binds and cleaves DNA is unimportant for reporting valid binding information for the drug. While DNase I catalyzes a phosphodiester hydrolysis of the DNA backbone, the porphyrin cleaves DNA via an oxo intermediate which appears to attack the deoxy-ribose moiety of the polymer. It is the specificity of the probe and not its mechanism of binding or cutting, per se, which needs to be addressed in obtaining information on site occupancy in the quantitative experiment. This point has recently been reinforced by preliminary results of quantitative footprinting experiments involving Fe-MPE (Dabrowiak and Goodisman, unpublished results). This intercalating complex cleaves DNA via radical release but, like DNase I, exhibits relatively low DNA sequence specificity. Despite the dramatic differences in cleavage mechanism, both the enzyme and Fe-MPE can be analyzed with the DNase I type redistribution model to yield valid binding constants for ligands bound to DNA.

When carrier DNA is present in excess, as is the case for the results considered here, it serves as a buffer for both drug and probe. While its presence in the experiment was initially viewed as a complication, it allows the determination of netropsin binding constants,  $K_i$ , without direct knowledge of the parameter  $K_p$ , the porphyrin binding constant toward its interaction sequences. The values of the  $K_i$  as well as the mean-square deviation  $D$  (Figure 9) are independent of  $K_p$  for  $K_p > \sim 10^6 \text{ M}^{-1}$ .

As before (Ward et al., 1988a), the binding of drug to DNA was assumed to occur in an independent noncooperative fashion. This assumption was included in the model used for analysis for two reasons. First, netropsin is a groove-binding drug, and unlike intercalators, it binds without greatly distorting DNA. Without distortion the possibility that affinities for adjacent binding sites would be altered through allosteric effects was considered remote. Also, only the early loading events on the polymer were used in the analysis. Thus, although many strong netropsin sites are present on the 139-mer, only a relatively small fraction of the fragments present in the reaction medium possess more than one bound drug molecule in the concentration range studied.

Although the porphyrin concentration used in the work was relatively low, about one porphyrin per fragment, the possibility exists that porphyrins bound to nearby drug sites would influence the binding constant of the drug for those sites. However, the generally good agreement between binding constants derived from DNase I and MnT4MPyP, which have radically different binding mechanisms, suggests that the porphyrin–drug cooperative effects are probably small and not detectable with the present data. A possible exception may be the site at 89 which is flanked by two porphyrin binding



sites. Occupancy of these flanking sites by MnT4MPyP may produce a distortion within the netropsin site causing the binding constant for this site to be lower than that obtained with DNase I, Table I.

The method described in this paper utilizes only the autoradiographic spot intensities derived from footprinting experiments and certain easily measured concentrations to determine drug binding constants as a function of sequence on natural DNA. The success of the approach depends on collecting intensity data for many sites on a DNA polymer. Since the number of experimental points is much larger than the number of parameters (binding constants) characterizing the loading events, a minimization approach can be used to calculate individual-site binding constants for ligands. Although the full scope and limitations of quantitative footprinting are yet to be defined, the method is clearly superior to conventional techniques which yield average rather than site-specific isotherms for ligand binding to a DNA lattice.

#### ACKNOWLEDGMENTS

We thank Professor B. R. Ware for helpful discussions concerning certain aspects of the work.

#### SUPPLEMENTARY MATERIAL AVAILABLE

Appendixes 1 and 2 discussing errors in quadratic fits and the analysis of the equilibrium involving the carrier DNA (7 pages). Ordering information is given on any current masthead page.

**Registry No.** MnT4MPyP, 70649-54-6; netropsin, 1438-30-8.

#### REFERENCES

- Bortolini, O., Ricci, M., Meunier, B., Friant, P., Ascone, L., & Goulou, J. (1986) *Nouv. J. Chim.* 10, 39.  
 Brenowitz, M., Senear, D. F., Shea, M. A., & Ackers, G. K. (1986a) *Methods Enzymol.* 130, 132-1819.  
 Brenowitz, M., Senear, D. F., Shea, M. A., & Ackers, G. K. (1986b) *Proc. Natl. Acad. Sci. U.S.A.* 83, 8462-8466.  
 Calladine, C. R. (1982) *J. Mol. Biol.* 161, 343-352.  
 Carey, J. (1988) *Proc. Natl. Acad. Sci. U.S.A.* 85, 975-979.  
 Chuprina, V. P. (1987) *Nucleic Acids Res.* 15, 293-311.  
 Dabrowiak, J. C., Skorobogaty, A., Rich, N., Vary, C. P. H., & Vournakis, J. N. (1986) *Nucleic Acids Res.* 14, 489-499.

- Fletcher, R. (1980) *Practical Methods of Optimization*, pp 14-15, Wiley, Chichester, U.K.  
 Geacintov, N. E., Ibanez, V., Rougee, M., & Bensasson, R. V. (1987) *Biochemistry* 26, 3087.  
 Goodisman, J., & Dabrowiak, J. C. (1985) *J. Biol. Struct. Dyn.* 2, 967-979.  
 Groves, J. T., & Nemo, T. E. (1983a) *J. Am. Chem. Soc.* 105, 5786.  
 Groves, J. T., & Nemo, T. E. (1983b) *J. Am. Chem. Soc.* 105, 6243.  
 Hurley, L. H., & Boyd, F. L. (1987) *Annu. Rep. Med. Chem.* 22, 259-268.  
 Kuwabara, M., Yoon, C., Goyne, T., Thederahn, T., & Sigman, D. S. (1986) *Biochemistry* 25, 7401-7407.  
 Lown, J. W., Sondhi, S. M., Org. C.-W., Skorobogaty, A., Kishikawa, H., & Dabrowiak, J. C. (1986) *Biochemistry* 25, 5111-5117.  
 Maniatis, F., Fritsch, E. F., & Sambrook, J. (1982) *Molecular Cloning—A Laboratory Manual*, Cold Spring Harbor, Cold Spring Harbor, NY.  
 Marky, L. A., & Breslauer, K. J. (1987) *Proc. Natl. Acad. Sci. U.S.A.* 84, 4359-4363.  
 Marmer, J., & Doty, P. (1962) *J. Mol. Biol.* 5, 109-118.  
 Raner, G., Ward, B., & Dabrowiak, J. C. (1988) *J. Coord. Chem.* 19, 17-23.  
 Raner, G., Ward, B., Goodisman, J., & Dabrowiak, J. C. (1989) *ACS Symposium Series*, American Chemical Society, Washington, DC (in press).  
 Senear, D. F., Brenowitz, M., Shea, M. A., & Ackers, G. K. (1986) *Biochemistry* 25, 7344-7354.  
 Suck, D., Lahm, A., & Oefner, C. (1988) *Nature* 332, 465-468.  
 Ward, B., Skorobogaty, A., & Dabrowiak, J. C. (1986) *Biochemistry* 25, 6875-6883.  
 Ward, B., Rehfuess, R., & Dabrowiak, J. C. (1987) *J. Biomol. Struct. Dyn.* 4, 685-695.  
 Ward, B., Rehfuess, R., Goodisman, J., & Dabrowiak, J. C. (1988a) *Biochemistry* 27, 1198-1205.  
 Ward, B., Rehfuess, R., Goodisman, J., & Dabrowiak, J. C. (1988b) *Nucleic Acids Res.* 16, 1359-1369.  
 Winter, R. B., & von Hippel, P. H. (1981) *Biochemistry* 20, 6948-6960.